scientific reports



OPEN

Mechanism of retinal angiogenesis induced by HIF-1 α and HIF-2 α under hyperoxic conditions

Xiaoxiao Feng^{1,2}, Changhui Li^{1,2,3}, Wenjia Zhang^{1,2}, Kangwei Jiao^{1,2}, Liwei Zhang^{1,2} & Libo Xiao^{1,2,4⊠}

In retinopathy of prematurity (ROP), preventing avascular dysplasia may be more critical than inhibiting abnormal neovascularization. While hypoxia-inducible factors (HIFs) are implicated in angiogenesis, their role in preventing ROP remains unclear. Oxygen-induced retinopathy (OIR) model and hyperoxic cell model were used in this study. Immunofluorescence, western blot, ELISA, cell counting kit-8 (CCK-8), and flow cytometry were applied to assess the effects of hyperoxia on the astrocytes. Co-culture of astrocytes with retinal microvascular endothelial cells (RMECs) was used to observe the effects of astrocyte inactivation on the RMECs. Overexpression of HIFs in astrocytes was used to investigate the mechanism. The OIR model revealed a decreased number of retinal astrocytes and the expression of dystrophin and R-cadherin in hyperoxic environments (P12), which was reversed after room air rearing (P17-P21), with an upward trend in RMECs (P21). In vitro hyperoxia induced significant apoptosis in astrocytes at 24 h. Moreover, the expression of angiogenesisrelated factors (VEGF and ANGPTL4), vascular stabilization, and development-related factors (Laminin-β2, Dystrophin, R-cadherin) was decreased. Co-culture of astrocytes and RMECs yielded similar conclusions, with astrocyte inactivation decreasing the tube-forming capacity of RMECs. Overexpression of HIFs in astrocytes promoted the expression of VEGF, ANGPTL4, and Laminin-β2 under hyperoxic conditions. Emphatically, HIF- 1α was more effective than HIF- 2α in promoting the expression of integrin β1, dystrophin, and R-cadherin. Overexpression of HIFs in astrocytes reverses hyperoxia-induced retinal astrocyte inactivation and retinal vascular structural disruption and dysplasia. Strikingly, HIF- 1α is a more suitable therapeutic target for ROP prevention than HIF- 2α .

Keywords Retinopathy of prematurity, Hypoxia-inducible factor, Retinal angiogenesis, Astrocytes, Oxygen-induced retinopathy

Retinopathy of prematurity (ROP) is a retinal vasoproliferative disease usually occurring in preterm infants with low gestational age and low birth weight. Despite improvements in the management of newborns, ROP remains the leading cause of childhood blindness worldwide. Studies found that the prevalence of ROP was as high as 68% in infants weighing < 1251 g¹. The initial emergence of ROP arose from the supplementation of oxygen in closed incubators to improve the survival of preterm infants². ROP can be divided into two phases. The first stage is the inhibition of angiogenic growth-associated factors by hyperoxia, resulting in the cessation of retinal vascular growth and the loss of existing retinal blood vessels3. Poorly vascularized retinas enter the second stage of ROP when oxygen transport is impaired, becoming hypoxic. This phase is characterized by compensatory vascular proliferation with poor perfusion of neovessels, leading to retinal detachment in severe cases. This was consistent with previous findings that hyperoxia in the oxygen-induced retinopathy (OIR) model resulted in retinal avascular dysplasia in mice, whereas neovascularization was resumed upon restoration of room air rearing⁴. The above findings suggest that the control of oxygen levels may be an effective strategy for preventing ROP. Additionally, our previous study found a strong correlation between the polarization of astrocytes and the changes in blood vessels during ROP5. Moreover, previous studies have found that astrocytes were connected to human retinal microvascular endothelial cells (RMECs) through protrusions to form an important structure of the intraretinal blood-retinal barrier (iBRB). The iBRB plays an important role in the stability of retinal microvessels and the regulation of angiogenesis^{6–8}. Dysfunction of astrocytes was a major cause of iBRB injury and retinal vascular disease⁶. Hence, we hypothesized whether it is possible to alter the behavior of astrocytes

¹Affiliated Hospital of Yunnan University, Kunming, China. ²Yunnan ophthalmic disease clinical medical center, Kunming, China. ³Kunming Medical University, Kunming, China. ⁴Department of Ophthalmology, Affiliated Hospital of Yunnan University, No.176 Qingnian Road, Kunming 650021, Yunnan, China. [⊠]email: fengxx@ynu.edu.cn

by controlling oxygen levels to prevent ROP. For this purpose, it might be effective to implement treatments to promote angiogenesis or inhibit avascular dysplasia during the first stage of ROP, in attempts to prevent hypoxia due to vascular dysplasia and thus enter the second stage of ROP.

Vascular endothelial growth factor (VEGF) has attracted extensive attention from researchers and has been used as a target for drug development for ROP therapy. Unfortunately, therapies designed to target VEGF have limited therapeutic efficacy in applications $^{9-12}$. Hypoxia-inducible factors (HIFs) have attracted our interest as regulated VEGF transcription factors. HIFs are heterodimeric proteins consisting of an oxygen-sensitive alpha subunit and a ubiquitous beta subunit 13,14 . HIF- α consists of three types, namely HIF- 1α , HIF- 2α , and HIF- 3α . Among them, HIF- 1α and HIF- 2α are highly homologous with similar structural domains, sharing 48% of the amino acid sequence 15 . Under specific conditions, HIF- 1α and HIF- 2α activate the transcriptional activity of multiple genes, such as VEGF, and play important roles in angiogenesis $^{16-18}$. Besides, at present, the role of HIF- 3α is not clearly defined. It is thought to be a selective splice isoform of HIF that negatively regulates HIF- 1^{9-21} . It has been shown that HIFs, which were usually expressed at low levels as mRNAs under physiological conditions, play an important role in maintaining retinal function and oxygen concentration within the retina. Notably, HIFs activation and translation were tightly regulated to support normal angiogenesis, which was essential for the treatment of ROP²²⁻²⁴. These studies suggest that HIFs may be a safer and more effective therapeutic target for the prevention of ROP with research significance.

This study aimed to examine the role of HIFs in ROP with the OIR animal model and hyperoxic cell model. The cell models have also been used to explore whether overexpression of HIFs under hyperoxic conditions promotes angiogenesis and development, leading to positive therapeutic effects in ROP.

Methods

Experimental animals and OIR animal model

C57BL/6 mice were obtained from the Experimental Animal Center of Kunming Medical University (License: SCXK (Dian) 2020-0004). These mice were randomly divided into 10 groups (n=6). Rearing conditions and the OIR model were as in the previous study⁴. Briefly, the P0 mice were kept at 21% O_2 for 7 days (P7), and then the P7 mice in the OIR group were kept at 75% O_2 for 5 days (P7-P12) to induce retinal avascular dysplasia. Finally, P12 mice in the OIR group were returned to 21% O_2 for 9 days (P12-P21) to induce retinal vascular neovascularization. Mice in the RA group were kept at 21% O_2 from P0 to P21. The oxygen concentration was strictly controlled to be maintained at 75%±2% throughout the hyperoxia experiment with an animal hyperoxia experiment system (Ox-100HE-S, Shanghai Tawang Intelligent Technology Co., Ltd., China). The mice were deeply anesthetized by intraperitoneal injection of pentobarbital sodium (120 mg/kg) at each sampling time point and subsequently euthanized by cervical dislocation. The retinas (without cornea, sclera, lens, vitreous, and vitreous vessels) were removed for subsequent experiments. Among them, 3 mice were randomly selected from each group for retinal section preparation, and the remaining ones were used for molecular detection. This study was approved by the Ethics Committee of Kunming Medical University (Kmmu20231525) and was conducted according to the ARRIVE guidelines. We confirm that all experiments were performed in accordance with relevant guidelines and regulations.

Cell culture and processing

Mouse retinal astrocytes (CP-R379, Punosai, China) were cultured under room air and hyperoxic conditions for 6 h, 12 h, and 24 h, respectively. The room air group is named RA, and the hyperoxic group is named HO. RA culture conditions were as follows: cells were cultured in AGM Bullet Kit culture medium (PNS CM-R379, Punosai, China) containing 1% P/S (gibco 15140-122, Thermo fisher, USA), and the dishes were placed in an incubator with 5% CO₂ and 95% air at 37 °C. HO was intervened by replacing the culture medium with serum-free and sugar-free ABM basal medium containing 1% P/S (Gibco 15140-122, Thermo Fisher, USA) and incubated in a triple-air cell culture incubator (75% O₂, 5% CO₂, 20% N₂, and 37 °C).

Co-culture of astrocytes and RMECs

To observe the effect of retinal astrocyte inactivation on RMECs, we co-cultured the two types of cells using both contact and non-contact methods. They were removed for evaluation at 6 h, 12 h, and 24 h of room air and hyperoxic culture. Contact co-culture better mimics the in vivo physiological state. The culture method was simply to first inoculate RMECs in DMEM culture medium containing 10% FBS (Gibco 10270-106, Thermo Fisher, USA) and 1% P/S (Gibco 15140-122, Thermo Fisher, USA). An additional 2 μL of PKH26 solution (P9691, Sigma, Germany) was added to 500 μL of RMECs suspension to label REMCs, and an additional 2 μL of Vybrant™ DiO cell labeling solution (Invitrogen, USA) was added to 500 μL of astrocyte suspension to label astrocytes. The slide covered with astrocytes was placed into RMEC culture dishes when the RMECs reached 80% area of the dish. The resultant cell supernatant was used for ELISA. The slides covered with astrocytes were removed and subjected to Western blot. The room air group was named Co-RA, and the hyperoxia group was named Co-HO. Additionally, non-contact culture was used in our experiments to exclude the complications and disturbances that may be caused by contact culture. RMECs were counted and inoculated in 12-well plates at 2×10^5 cells per well. The astrocytes were inoculated at 1×10^5 cells per well in a 12-well plate transwell. After 12 h of room air incubation, the transwells were placed into 12-well plates for co-culture. At the end of the culture, CCK-8 and angiogenesis assays were performed on RMECs. The room air culture group was named CO-RA, and the hyperoxia culture group was named CO-HO.

Immunofluorescence (IF) staining

Retinal Sect. 8 μ m thick were prepared using a slicer (Leica, Germany) from RA and OIR groups at stages P12, P17, and P21. Each group had three mice at each time point (n=3), and the right retina of each mouse was

2025 15:36049

Scientific Reports |

used to prepare sections. Each section was photographed in three fields of view (n=3). The retinal sampling site was the peripapillary region (Centered on the optic nerve head (ONH), within a radius of approximately 0.1–0.7 mm). Cell crawls (n=3) from RA and HO groups were fixed utilizing 4% paraformaldehyde (Lightfast, China). Sections or crawls to be tested were permeabilized with 3% Triton-X 100, closed with 5% goat serum, and then incubated with primary antibodies CD31 (1:300, ab9498, Abcam, USA), GFAP (1:250; ab4648, Abcam, USA), HIF-1 α (1:300, 20960-1-AP proteintech, USA), HIF-2 α (1:200, 26422-1-AP, proteintech, USA), PAX-2 (1:100, 29307-1-AP, proteintech, USA), Laminin- β 2 (1:200, bs-7504R, bioss. China) and Dystrophin (1:100, 12715-1-AP, proteintech, USA). After washing, secondary antibodies Affinity-purified antibody Cy3-labeled goat Anti-rabbit IgG (H+L) (1:1000, 072-01-15-06, KPL, USA) and Affinity-purified Antibody Daylight 488 Labeled Goat anti-Mouse IgG (H+L) (1:1000, 5230 – 0391, KPL, USA) were incubated. Scanning and photography were performed using a panoramic scanning system (3D HISTECH, Hungary) and a BX53 microscope (Olympus, Japan). IF intensities were all quantified by using Image J software.

Western blot

RIPA lysate (P0013B, Biyun Tian, China) was used to extract proteins from retinal tissues or astrocytes. After protein quantification, 60 μ g per well was used for SDS-PAGE electrophoresis. After membrane transfer, these membranes were blocked at room temperature using 5% skimmed milk for 1 h. Subsequently, 5 mL of primary antibodies β -actin (1:4000, TA-09, Zhongshanjinqiao, China), GFAP (1:10000, 16825-1-AP, proteintech, USA), Laminin- β 2 (1:12000, 30943-1-AP, proteintech, USA), Dystrophin (1:10000, 12715-1-AP, proteintech, USA), R-cadherin (1:1000, 19795-1-AP, proteintech, USA) and integrin β 1 (1:2000, 26918-1-AP, proteintech, USA) was added and incubated at 4 °C overnight. Subsequently, incubation with enzyme-labeled secondary antibodies, Goat Anti Mouse IgG-HRP (1:4000, M21001L, Abmart, China), Goat Anti Rabbit IgG-HRP (1:4000, M21002L, Abmart, China) was performed at room temperature for 2 h. After washing, the ECL kit (P0018S, Abmart, China) was used for luminescence detection.

CCK-8

Trypsin (0.25%, Gibco 1894145, Thermo Fisher, USA) was used to collect cells. Cells were centrifuged and resuspended, and 100 μ L was added to 96-well plates. To each well, 10 μ L of CCK-8 solution (CK04, Tongren Chemistry, China) was added, and the OD value of each well was detected at 450 nm after incubation for 2 h at room temperature and protected from light. The cell viability of each well was calculated based on the OD value.

Flow cytometry using annexin V staining

The cell suspension was centrifuged at 1000 rpm/min for 3 min to collect the cells and resuspended. Apoptosis was detected according to the instructions of the Apoptosis Detection Kit (A004, Seven Seas Bio, China). A blank control, FITC single positive control, and PI single positive control were also set to exclude interference. FITC-/PI- represents live cells; FITC+/PI- represents early apoptotic cells; FITC+/PI- represents late apoptotic cells; FITC-/PI- represents necrotic cells. Total apoptosis was the sum of early apoptotic cells and late apoptotic cells.

ELISA

Cell supernatants were diluted 5-fold and assayed according to the instructions of the Mouse Angiopoietin-like Protein 4 (ANGPTL4) Kit (JL18884, Elabscience, China) and Mouse Vascular Endothelial Growth Factor A (VEGFA) Kit (E-MSEL-M0005, Elabscience, China). OD values were measured at 450 nm within 15 min of reaction termination using an EL800 enzyme labeling instrument (BIO-TEK, USA).

Vessel formation assay

Melted Matrigel (356232, Corning, USA) was mixed with an equal amount of pre-cooled basal medium at 4 $^{\circ}$ C on an ice box and spread in 24-well plates. Subsequently, the cells were cultured for 30 min at 37 $^{\circ}$ C. After cell counting, 500 μ L of cell suspension with a concentration of 2×10⁵ cells /mL was spread evenly in the chambers with Matrigel, mixed well, and returned to the incubator for 5–6 h for observation.

Lentiviral vector construction and lentiviral transfection of astrocytes

Lentiviral vector construction was done by Genomeditech. The vectors used were PGMLV-CMV-MCS-EF1-mScarlet-T2A-Puro. Overexpression vectors of HIF-1 α and HIF-2 α were obtained after primer design, vector biallelic cleavage, target gene amplification, ligation, transformation, and sequencing. After lentiviral packaging and titer assay, we obtained the required lentiviral vectors. The titer of HIF-1 α overexpression lentivirus was 1.11×10^8 TU/mL, and the titer of HIF-2 α overexpression lentivirus was 3.08×10^7 TU/mL. Western blot and RT-qPCR were used to verify the expression of lentiviral vectors.

Lentiviral transfection and treatment of astrocytes: Astrocytes were inoculated in 24-well plates at a density of 1×10^4 cells/well, and lentiviral transfection was performed when the cell density reached 40%. In each group, 5 μ L of medium, lentiviral empty vector, HIF-1 α , or HIF-2 α overexpression lentivirus was added and cultured in an incubator for 48 h. The groups were named Con, NC-1/2, OE-HIF1 α , and OE-HIF2 α , respectively. Then, the cells of the OE-HIF1 α and OE-HIF2 α groups were cultured in hyperoxia for 24 h, and named O-HIF1 α and O-HIF2 α . The supernatants were collected for ELISA, and the cells were collected for western blot and IF.

RT-qPCR

Trizol Reagent (15596026, Lifetech, China) was used to extract RNA from the cells. The EzDrop1000 Spectrophotometer (Blue-ray bio, China) was used to calculate the concentration of RNA. The cDNA was synthesized according to the instructions of the FastKing RT Kit (With gDNase) kit (KR116, Tiangen, China).

Scientific Reports |

Taq Pro Universal SYBR qPCR Master Mix (Vazyme, China) was used for amplicon quantification. The results were analyzed by the $2^{-\triangle\triangle Ct}$ method. β -actin was used as an internal reference gene. Primer information is shown in Table 1.

Statistical analysis

All experiments were repeated at least three times, and data were statistically analyzed and visualized using SPSS 23.0 and Origin 2021. Data are expressed as mean \pm SD of parallel independent experiments. Statistical probability was assessed using a One-Way ANOVA analysis of variance, and the data were further compared between the two groups using the LSD method. p < 0.05 indicates a statistically significant difference.

Results

Relationship between retinal astrocytes and retinal vascular development in the OIR model

Our previous studies have shown that polarization of retinal astrocytes plays an important role in avascular dysplasia (P7-P12) and neovascularization (P17-P21) in the retina⁵. In this study, the immunostaining levels of GAFP-labeled astrocytes and HIFs showed a significant decrease at P12 and gradually recovered after rearing in room air (P17-P21) (Figs. 1 and 2A,B). These findings suggested that HIF-1a and HIF-2a were positively associated with angiogenesis. RMECs were fluorescently labeled with CD31 to observe changes. The results showed a significant decrease at P12 and gradually recovered after rearing in room air (P17-P21). It is noteworthy that CD31 increased significantly at P21 (Fig. 2A,B), suggesting that the return of mice from a hyperoxic environment to a room air environment induced compensatory proliferation of retinal blood vessels. Subsequent western blot results showed that astrocytes in the OIR model were significantly lower than those in RA at the end of hyperoxia (P12), despite elevated astrocyte counts during the subsequent room air rearing phase (P17), until P21 returns to its normal value (Fig. 2C). Dystrophin was a marker of skeletal muscle cell membranes and had a stabilizing effect on vascular structure²⁵. R-cadherin was a retinal calmodulin that mediates adhesion between retinal neurons and was essential for retinal development and structural maintenance²⁶. In this study, the expression of dystrophin and R-cadherin was similar to that of astrocytes. That was, after a hyperoxic environment (P12), a significant decrease in content was exhibited, which gradually recovered with room air rearing (P17 and P21) (Fig. 2D,E). These findings suggested that hyperoxic environments cause damage to the retinal vascular system, which gradually repairs upon return to the room air environment.

Hyperoxia causes inactivation of retinal astrocytes

To further investigate retinal astrocytes in a hyperoxic environment, we incubated retinal astrocytes in room air (RA) and hyperoxic (HO) environments, respectively. Retinal astrocytes were removed at 6 h, 12 h, and 24 h and evaluated. CCK-8 results showed that the cell viability of astrocytes in the HO group was significantly lower (Fig. 3A) and the apoptosis was significantly higher (Fig. 3B) than that of RA at 24 h. PAX-2 was a key factor in embryonic retinal development²⁷. PAX-2 was specifically expressed in retinal astrocytes and their precursor cells (APCs), and GFAP/PAX-2-labeled cells were used to indicate the astrocytes²⁸. Immunofluorescence results revealed a significant decrease in PAX-2 at 12 h and 24 h in the HO group (Fig. 3C). Moreover, in the HO condition, astrocytes showed stressful elevated (elevated GFAP/PAX-2 expression) at 6 h and gradually decreased with time until they were significantly lower than those in the RA group at 24 h (Fig. 3C). Angiopoietin-like protein 4 (ANGPTL4) and VEGF were key factors in inducing retinal neoangiogenesis 29,30. ELISA assay revealed a significant decrease in ANGPTL4 at 12 h of hyperoxia. Subsequently, at 24 h, both ANGPTL4 and VEGF were significantly lower in the HO group than in the RA group (Fig. 3D,E). From these results, it was found that hyperoxia-treated astrocytes showed significant inactivation at 24 h. Subsequently, the western blot was performed on the cells at 24 h. The results showed that the protein expression of HIF-1a, HIF-2a, Dystrophin, R-cadherin, and Laminin-β2 was significantly decreased in the HO group (Fig. 3F-J). Laminin-β2 supported the differentiation of neural ectodermal cells, such as retinal pigment epithelial cells and photoreceptors, and had an important role in retinal development³¹. These findings suggested that decreased viability and apoptosis of astrocytes have a range of adverse effects on the retina, including angiogenesis, impaired retinal development, and structural damage.

Inactivation of retinal astrocytes induces dysfunction of RMECs

To further investigate the effect of astrocytes on RMECs, contact and non-contact co-cultures were applied. Contact co-culture of astrocytes and RMECs (Fig. 4A) revealed a significant decrease in ANGPTL4 and VEGF expression in the hyperoxia group (Co-HO) at 24 h (Fig. 4B,C). Additionally, integrin β 1 regulates cell adhesion, migration, and proliferation, and has an important role in angiogenesis and maintenance of stability³². Our research found that protein expression of integrin β 1 and Laminin- β 2 in astrocytes in the Co-HO group was significantly lower than that in the Co-RA group at 12 h and 24 h (Fig. 4D,E). These results suggested that hyperoxia leads to impaired angiogenesis and decreased stability. In non-contact co-culture, the cell viability

	F (5'-3')	R (5'-3')
β-actin	CTGGAGAAGAGCTATGAG	GATGGAATTGAATGTAGTTTC
HIF-1α	TGTTGTAAGTGGTATTATTC	CTTGTATCCTCTGATTCA
HIF-2α	ACTTACTCAGGTAGAACTAACAG	TCTCACGGATCTCCTCAT

Table 1. Primer information.

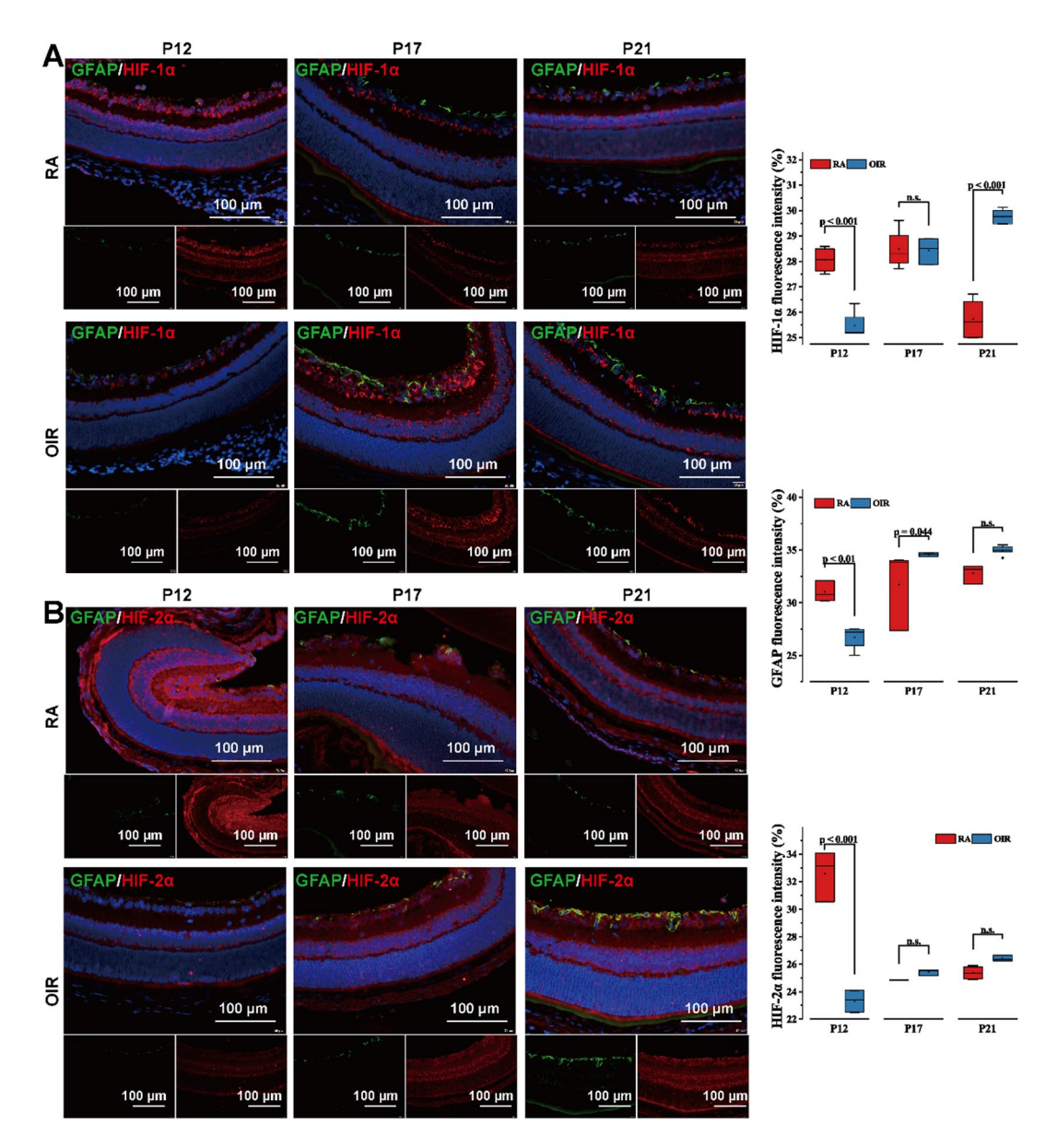


Fig. 1. Changes of astrocytes and HIFs in the OIR model. (A, B) IF staining was used to visualize GFAP-labeled astrocytes (green), HIF-1 α (A, red), and HIF-2 α (B, red) in the retinas of C57BL/6 mice at P12, P17, and P21; Scale bar: 100 μ m. p < 0.05 was considered a significant difference, and n.s. means the difference was not significant. The data of RA and OIR groups at stages P12, P17, and P21 (n = 3) were obtained through at least three independent repeated experiments.

of RMECs in the hyperoxia group (CO-HO) decreased significantly at 24 h (Fig. 4F). Furthermore, in the CO-HO group, the endothelial cell tube appeared to be partially fractured at 6 h and dispersed at 24 h, making it difficult to visualize the lumen morphology (Fig. 4G). These findings suggested that inactivation of astrocytes induces a decrease or even loss of angiogenesis and luminal barrier maintenance function of RMECs through the regulation of angiogenesis and maintenance of stability-related signaling factors.

HIFs modulate the orientation of retinal astrocytes

HIFs were observed to be affected by oxygen content in both OIR and cellular models and were associated with retinal angiogenesis and stabilization. HIFs play a key role in retinal vasculopathy. Overexpression of HIF-1 α and HIF-2 α , typical members of HIFs, was performed on treated astrocytes (Fig. 5A–D) and cultured in a hyperoxic environment (Fig. 5E,F) to observe the regulatory effect of HIF overexpression on the expression of angiogenesis and development-related genes in astrocytes. The results showed that overexpression of HIF-1/2 α in a hyperoxic environment both significantly reversed the decrease in the content of ANGPTL4 and VEGF due to HO (Fig. 5G,H), and O-HIF1 α was more effective than O-HIF2 α . Moreover, O-HIF1 α significantly reversed the decrease in protein expression of Laminin- β 2, integrin β 1, dystrophin, and R-cadherin due to HO (Fig. 5I–L). O-HIF2 α failed to reverse the inhibitory effect of hyperoxia on integrin β 1, dystrophin, and R-cadherin

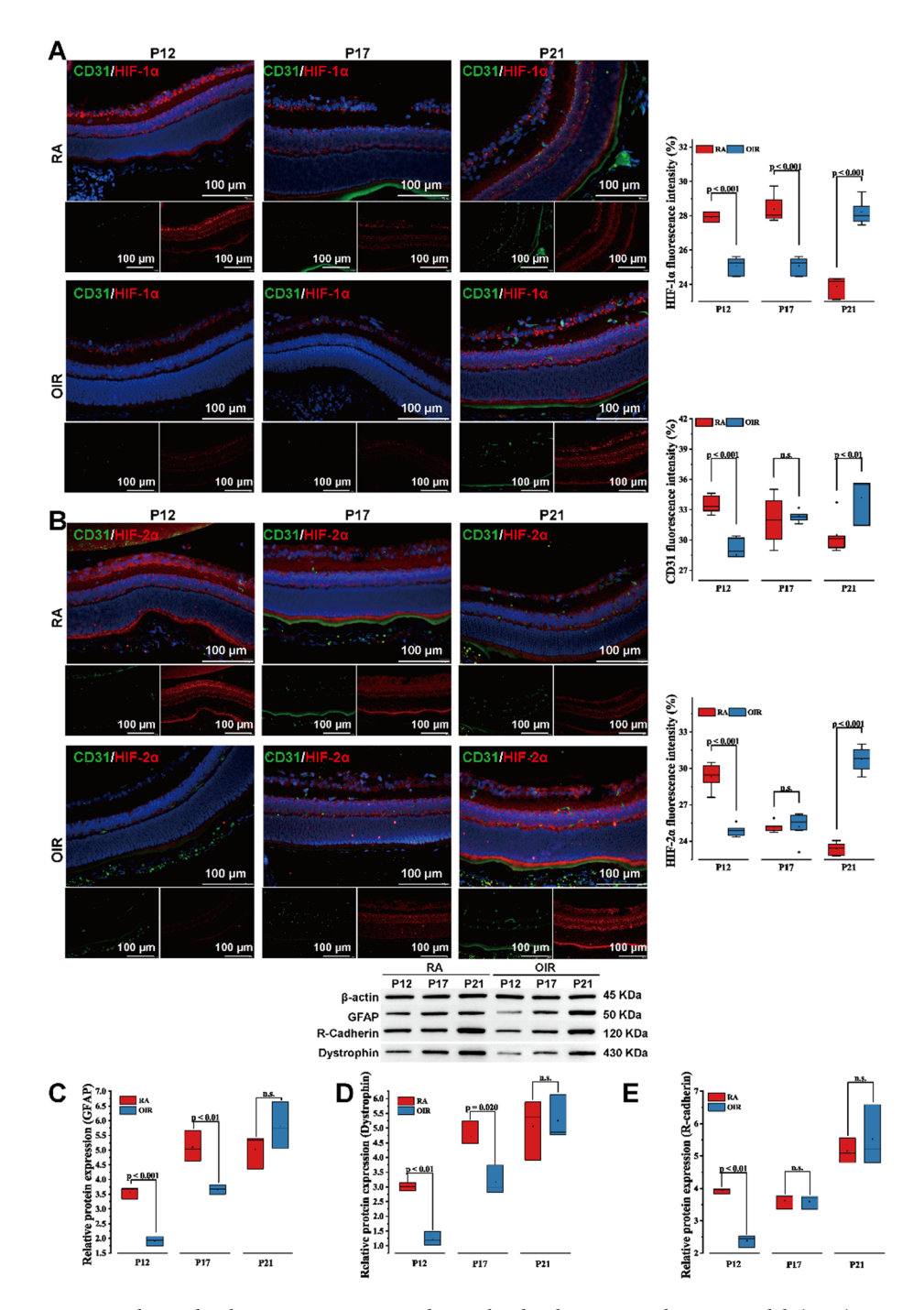


Fig. 2. Relationship between astrocytes and vascular development in the OIR model. (**A**, **B**) IF staining was used to visualize CD31 (green), HIF-1α (A, red), and HIF-2α (B, red) in the retinas of C57BL/6 mice at P12, P17, and P21; scale bar: 100 μm. (**C**-**E**) Western blot was used to visualize the protein expression of GFAP (C) and the vascular development-associated factors dystrophin (D) and R-cadherin (E) in the retinas of C57BL/6 mice at P12, P17, and P21. p < 0.05 was considered a significant difference, and n.s. means the difference was not significant. The data of RA and OIR groups at stages P12, P17, and P21 (n = 3) were obtained through at least three independent repeated experiments.

(Fig. 5J–L), but succeeded in doing so for Laminin- $\beta 2$ (Fig. 5I). IF assays demonstrated similar results (Fig. 5M). These results suggested that HIFs indeed modulate the ability of astrocytes to control angiogenesis and vascular stability, with a better positive directional effect of HIF-1 α than HIF-2 α .

Discussion

The OIR model was the definitive model for studying retinopathy^{33,34}. In our study, the OIR model showed a decrease in the number of astrocytes and in the expression of factors related to vascular structural stability

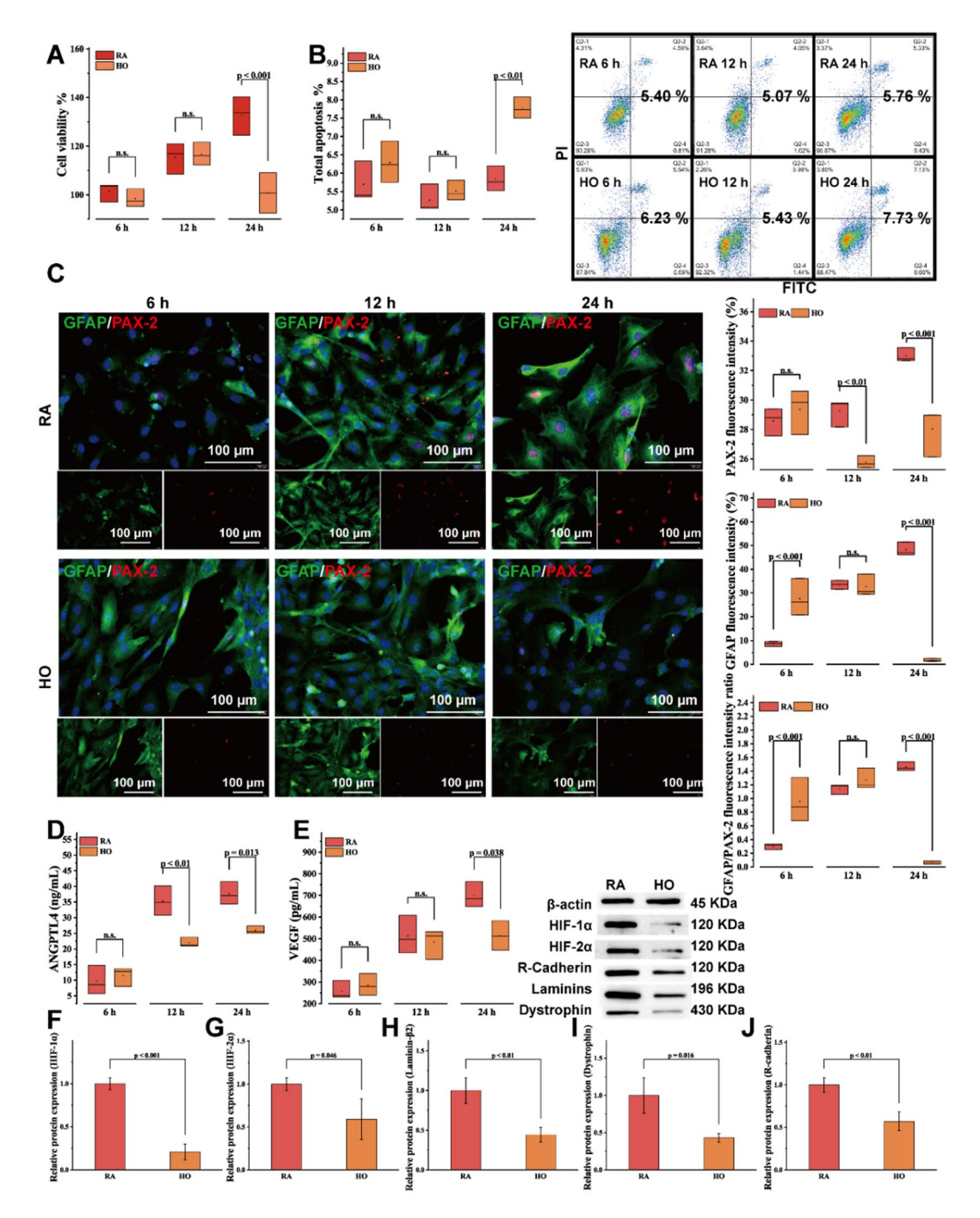


Fig. 3. Hyperoxia leads to retinal astrocyte inactivation. (A) CCK-8 was used to assess the viability of astrocytes. (B) Flow cytometry was used to detect astrocyte apoptosis. (C) IF staining was used to visualize activated state astrocytes at 6 h, 12 h, and 24 h; scale bar: 100 μ m; GFAP in green, PAX-2 in red. (D, E) ELISA was used to assess the levels of angiogenesis-related factors ANGPTL4(D) and VEGF(E) in astrocytes. (F–J) Western blot was used to visualize the protein expression of HIF-1 α (F), HIF-2 α (G), Laminin- β 2 (H), dystrophin (I), and R-cadherin (J) in astrocytes at 24 h of culture. p < 0.05 was considered a significant difference, and n.s. means the difference was not significant. The data of RA and HO groups at 6 h, 12 h, and 24 h (n = 3) were obtained through at least three independent repeated experiments.

(dystrophin and R-cadherin) at P12, which was reversed during the subsequent room air-rearing phase (P17-P21). Besides, the levels of CD31 immunofluorescence reflected a significant decrease in the number of RMECs at P12 and a significant increase in the number of RMECs at P21. These results were consistent with the phases of avascular dysplasia and subsequent neovascularization in the OIR model^{35–37}. In addition, previous studies focused on HIF-1 α and found that inhibition of HIF-1 α /VEGF signaling effectively alleviated pathological neovascularization in the retina^{38,39}. Differently, we observed the changes of HIF-2 α in astrocytes

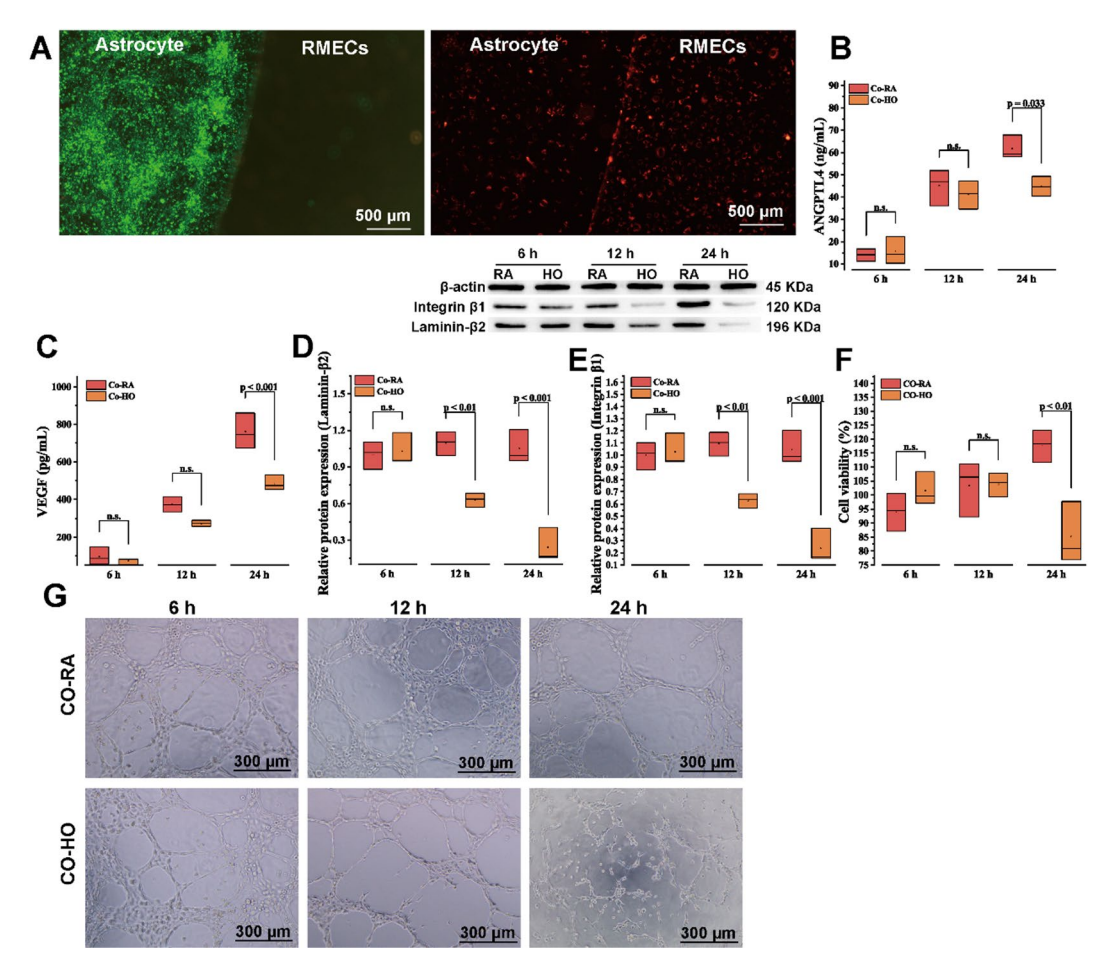


Fig. 4. Astrocyte inactivation leads to decreased function of RMECs. (A) Contact co-culture of astrocytes (green) with RMECs (red); scale bar: $500 \ \mu m$. (B, C) ELISA was used to assess the levels of angiogenesis-related factors ANGPTL4(B) and VEGF(C) in the supernatants of contact co-cultured cells. (D, E) Western blot was used to visualize the protein expression of Laminin- $\beta 2$ (D) and integrin $\beta 1$ (E) in contact co-cultured astrocytes. (F) CCK-8 was used to assess the cell viability of RMECs in non-contact co-culture. G: Lumen formation assay was used to observe the tube-forming ability; scale bar: $300 \ \mu m$. p < 0.05 was considered a significant difference, and n.s. means the difference was not significant. The data of RA and HO groups at 6 h, $12 \ h$, and $24 \ h$ (n = 3) were obtained through at least three independent repeated experiments.

and RMECs apart from HIF-1α and found that the changes in its expression were also stage-specific. These findings suggested the relevance of HIF-1α and HIF-2α to avascular dysplasia and neovascularization processes. Hyperoxia-induced decreases in retinal astrocytes have been noted for a long time in animal models³⁷. In our in vitro cellular experiments, a decrease in cell viability and an increase in apoptosis were similarly observed in retinal astrocytes at 24 h of hyperoxia. Moreover, the PAX-2 decreased significantly at 24 h of hyperoxia in this study. PAX-2 was a marker of early retinal APCs. APCs can differentiate into mature retinal astrocytes, and a decrease in GFAP/PAX-2 expression indicates the loss of astrocytes and severe damage to the optic nerve^{28,40,41}. Furthermore, we observed a decline in the expression of ANGPTL4, VEGF, dystrophin, R-cadherin, and Laminin-β2. Previous studies have found that Laminins were important for the maintenance of vascular stability by recruiting vascular basement membrane (BM) components. Moreover, integrin β1 and dystrophin were recognized as the main cellular anchoring receptors interacting with Laminin- $\beta 2^{42}$. Besides, the researchers found that retinal vascular development was mediated by endothelial filamentous pseudopods, which were both templates for astrocytes and specific R-cadherin²⁶. Moreover, previous studies have found that retinal astrocytes were a source of VEGF signaling, and retinal astrocytes contributed to ROP revascularization by secreting VEGF, acting on nearby endothelial cells (ECs)³⁰. These findings demonstrated that hyperoxia leads to inactivation and poor differentiation of retinal astrocytes. Decreased secretion of vascular stability and development-related factors promoted vasolysis and developmental inhibition. Furthermore, these research results suggested that the above-mentioned genes were HIF-dependent. Besides, the previous study of Duan et al. had shown that after 24 h of hyperoxia-treated mouse, an increase in astrocyte differentiation was observed, as evidenced by an increase in GFAP labeling and GFAP/PAX-2 ratio⁴³. Differently, at 24 h, we observed a significant decrease in PAX-2, GFAP and GFAP/PAX-2 in vitro. Such differences may be due to the fact that our experiments were in vitro, whereas the study of Duan et al. was an in vivo experiment. The in vitro experiments

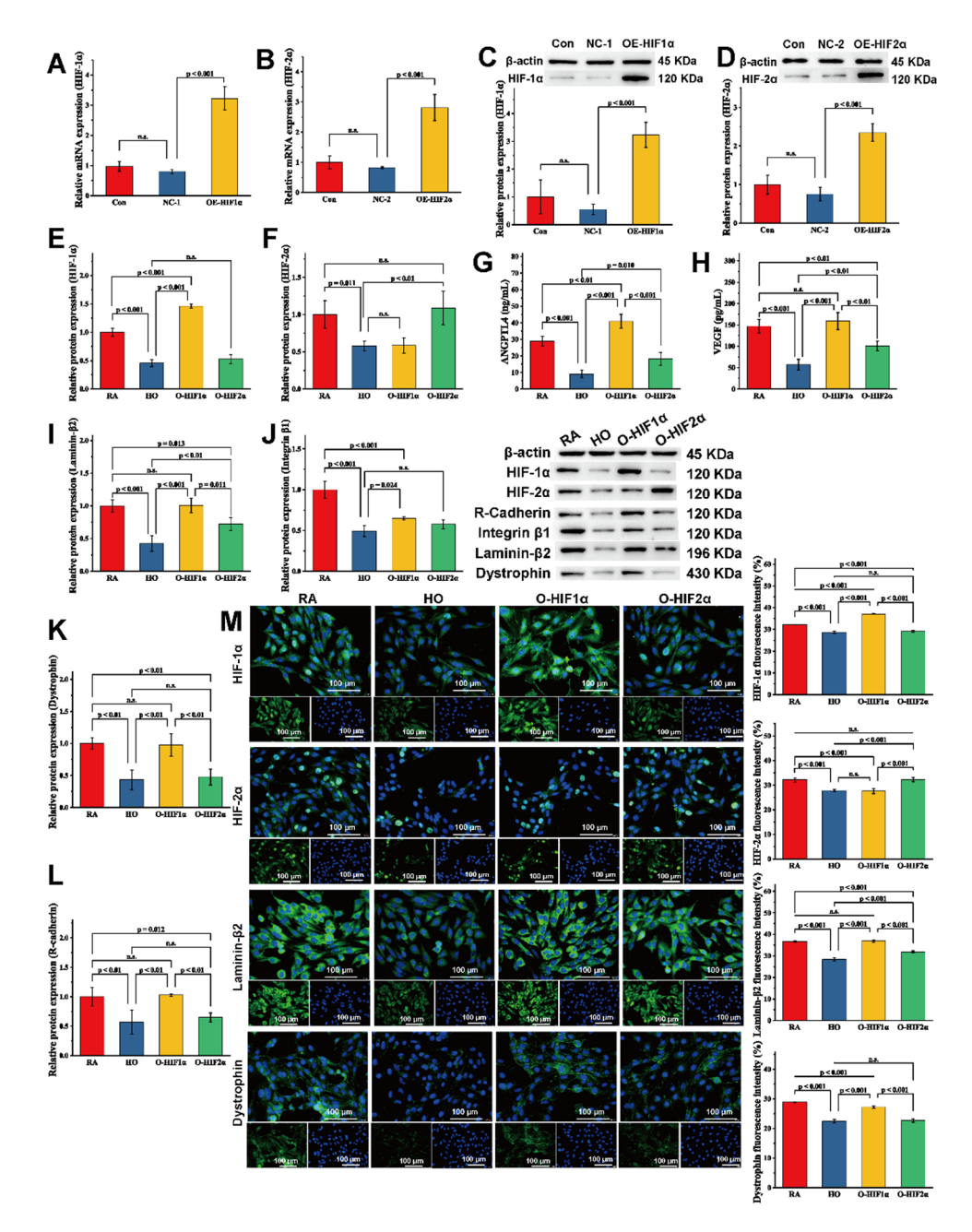


Fig. 5. Overexpression of HIFs promotes the vasculature-directed capacity of astrocytes. (**A**, **B**) RT-qPCR was used to evaluate the overexpression of HIF-1α (A) and HIF-2α (B) at the mRNA level. (**C**–**F**) Western blot was used to evaluate the overexpression of HIF-1α (C) and HIF-2α (D) under room air and the overexpression of HIF-1α (E) and HIF-2α (F) under hyperoxia. (**G**, **H**) ELISA was used to assess the levels of ANGPTL4 (G) and VEGF (H). (**I**–**L**) Western blot was used to assess the protein expression of Laminin-β2 (I), integrin β1 (J), dystrophin (K), and R-cadherin (L). (**M**) IF staining was used to visualize HIF-1α, HIF-2α, Laminin-β2, and dystrophin in astrocytes after overexpression of HIFs under hyperoxia. p < 0.05 was considered a significant difference, and n.s. means the difference was not significant. The data of each group (n = 3) was obtained through at least three independent repeated experiments.

are usually faster than the in vivo ones, which could well explain the results at 6 h in our in vitro experiments were consistent with the findings of Duan et al. This may be an acute compensatory increase, while the number of astrocytes begin to show a decline as the hyperoxic environment persists. Similarly, studies in the OIR mouse model found that the hyperoxic environment led to a decline in astrocyte numbers and a rebound with the restoration of the oxygen environment³⁷which was consistent with our results. Our in vivo experiments were conducted over a much longer period of time. During this period, the mice may have had more time for self-regulation. Therefore, the conclusions we reached were more convincing and reliable. Moreover, RMECs were the core cells that constitute the retinal vascular system. It is important to observe how astrocytes act on

RMECs to exert angiogenic regulation. In this study, a decrease in the expression of angiogenesis-related factors (ANGPTL4 and VEGF) in the supernatant and vascular stability-related factors (integrin β1 and Laminin-β2) in astrocytes was observed in contact co-cultured with hyperoxia for 24 h. This was in line with researchers who found that betaine acts as an anti-angiogenic agent by inhibiting VEGF signaling⁴⁴. Decreased cell viability of RMECs, along with breakage and disappearance of the vascular lumen, was observed in our noncontact coculture experiments under a hyperoxic environment. These results suggested that the action of retinal astrocytes on RMECs do not act through physical contact-dependent interactions, but rather through paracrine versus chemical signaling diffusion. In other words, retinal astrocytes directed RMECs by altering the secretion, expression of key cytokines (ANGPTL4, VEGF, Dystrophin, R-cadherin, Laminin-β2, and integrin β1), causing impaired vascular development and degradation of the existing vasculature. Notably, the trend of decreased or increased expression of HIF-1α and HIF-2α in oxygen-mediated animal and cellular models of ROP was consistent with the results of impaired angiogenesis or neovascularization. These results reaffirmed that HIFs play an important role in angiogenesis in ROP. Subsequently, we overexpressed HIF-1a and HIF-2a in astrocytes to investigate the mechanism of angiogenesis regulation by HIFs. Our results showed that overexpression of HIF-1α/2α under hyperoxia significantly reversed the decrease in ANGPTL4 and VEGF contents due to HO. Striking, HIF-1a demonstrated a better effect than HIF-2a. This was consistent with previous studies which found that inhibition of either HIF-1α or HIF-2α prevented neovascularization. HIF-1 alone was sufficient to promote retinal neovascularization, whereas therapies targeting only HIF-2 struggled to achieve the goal^{29,45}. The difference was that our findings on angiogenic factors may partially explain the reason. Overexpression of HIF-1α significantly reversed the HO-induced decrease in the expression of vascular stability and developmentrelated proteins. Whereas HIF-2 α exhibited a significant elevation only in Laminin- β 2. These findings suggested that HIF-1α affects vascular development and stability in more ways.

In summary, both HIF-1 α and HIF-2 α mediated neovascularization in a hyperoxic environment, and HIF-1 α is more powerful. This difference in ability may stem from the fact that HIF-1 α more effectively promotes the expression of angiogenic (ANGPTL4 and VEGF) and vascular development and stabilization-related factors (Laminin- β 2, Integrin β 1, dystrophin, and R-cadherin). In contrast, HIF-2 α promotes neovascularization and stabilization only by promoting the secretion of angiogenic factors and the recruitment effect of Laminin- β 2 expression. These findings suggested that HIF-1 α promoted angiogenesis and prevented neovascularization degradation, and was a better therapeutic target in the hyperoxic phase of ROP than HIF-2 α . However, our research results on the overexpression of HIFs were only explored in cells in vitro, and further animal experiments and clinical validation were needed. Nonetheless, this study still demonstrated that HIFs can be used as a preventive therapeutic target for ROP and contributed to the therapeutic mechanism exploration of ROP.

Conclusion

Hyperoxic environments lead to the inactivation of retinal astrocytes. The inactivated retinal astrocytes induce decreased expression of the angiogenesis-related factors ANGPTL4 and VEGF, and the vascular development- and stability-related factors Laminin- $\beta 2$, integrin $\beta 1$, dystrophin, and R-cadherin, which leads to a decreased viability of RMECs and destruction of the vessel wall. However, overexpression of both HIF-1 α and HIF-2 α in retinal astrocytes under hyperoxia effectively reversed the destruction caused by HO. Notably, HIF-1 α was more effective than HIF-2 α .

Data availability

All data generated or analyzed during this study are included in this published article. Data will be made available on request.

Received: 14 March 2025; Accepted: 11 September 2025

Published online: 15 October 2025

References

- 1. Good, W. V. et al. The incidence and course of retinopathy of prematurity: findings from the early treatment for retinopathy of prematurity study. *Pediatrics* 116, 15–23 (2005).
- 2. Richards, M. P. M. & Retrolental fibroplasia: A modern parable. By W. A. Silverman. (Grune \& Stratton, New York 1980) Price £13.20 (US \\$23.50). J. Biosoc. Sci. 13, 501–503 (1981).
- 3. Pierce, E. A., Foley, E. D. & Smith, L. E. Regulation of vascular endothelial growth factor by oxygen in a model of retinopathy of prematurity. *Arch. Ophthalmol. (Chicago, Ill. 1960)* 114, 1219–1228 (1996).
- 4. Smith, L. E. et al. Oxygen-induced retinopathy in the mouse. Invest. Ophthalmol. Vis. Sci. 35, 101-111 (1994).
- 5. Feng, X. et al. Tracking astrocyte polarization in the retina in retinopathy of prematurity. Exp. Eye Res. 250, 110170 (2025)
- 6. Deng, J. et al. The development of blood-retinal barrier during the interaction of Ast Rocytes with vascular wall cells. *Neural Regen Res.* 9, 1047 (2025).
- 7. Grinspan, J. B. et al. Rat brain microvessel extracellular matrix modulates the phenotype of cultured rat type 1 astroglia. *Dev. Brain Res.* 33, 291–295 (1987).
- 8. Sheng, X. et al. Microvascular destabilization and intricated network of the cytokines in diabetic retinopathy: from the perspective of cellular and molecular components. *Cell. Biosci.* 14, 85 (2024).
- 9. Seery, C. W. et al. Update on the use of Anti-VEGF drugs in the treatment of retinopathy of prematurity. *J. Pediatr. Ophthalmol. Strabismus.* 57, 351–362 (2020).
- Kurihara, T., Westenskow, P. D., Bravo, S., Aguilar, E. & Friedlander, M. Targeted deletion of Vegfa in adult mice induces vision loss. I. Clin. Invest. 122, 4213–4217 (2012).
- 11. Bakri, S. J. et al. Intraocular pressure in eyes receiving monthly Ranibizumab in 2 pivotal age-related macular degeneration clinical trials. *Ophthalmology* **121 5**, 1102–1108 (2014).

- 12. Grunwald, J. E. et al. Risk of geographic atrophy in the comparison of age-related macular degeneration treatments trials. *Ophthalmology* **121**, 150–161 (2014).
- 13. Semenza, G. L. Hypoxia-inducible factor 1 (HIF-1) pathway. Sci. STKE 2007 cm8 (2007).
- 14. Semenza, G. L. Targeting HIF-1 for cancer therapy. Nat. Rev. Cancer. 3, 721-732 (2003).
- 15. Keith, B., Johnson, R. S. & Simon, M. C. HIF1α and HIF2α: sibling rivalry in hypoxic tumour growth and progression. *Nat. Rev. Cancer.* 12, 9–22 (2011).
- 16. Semenza, G. L. Angiogenesis in ischemic and neoplastic disorders. Annu. Rev. Med. 54, 17-28 (2003).
- 17. Maxwell, P. H. & Ratcliffe, P. J. Oxygen sensors and angiogenesis. Semin Cell. Dev. Biol. 13, 29-37 (2002).
- 18. Forsythe, J. A. et al. Activation of vascular endothelial growth factor gene transcription by hypoxia-inducible factor 1. *Mol. Cell. Biol.* **16**, 4604–4613 (1996).
- 19. Makino, Y., Kanopka, A., Wilson, W. J., Tanaka, H. & Poellinger, L. Inhibitory PAS domain protein (IPAS) is a hypoxia-inducible splicing variant of the hypoxia-inducible factor-3alpha locus. *J. Biol. Chem.* 277, 32405–32408 (2002).
- 20. Duan, C. Hypoxia-inducible factor 3 biology: complexities and emerging themes. Am. J. Physiol. Cell. Physiol. 310, C260-C269 (2016)
- 21. Maynard, M. A. et al. Human HIF-3α4 is a dominant-negative regulator of HIF-1 and is down-regulated in renal cell carcinoma. *FASEB J.* **19**, 1396–1406 (2005).
- 22. Peet, D. J., Kittipassorn, T., Wood, J. P., Chidlow, G. & Casson, R. J. HIF signalling: the eyes have it. Exp. Cell. Res. 356, 136–140 (2017).
- 23. Hartnett, M. E. Advances in Understanding and management of retinopathy of prematurity. Surv. Ophthalmol. 62, 257-276 (2017).
- 24. Alon, T. et al. Vascular endothelial growth factor acts as a survival factor for newly formed retinal vessels and has implications for retinopathy of prematurity. *Nat. Med.* 1, 1024–1028 (1995).
- Giocanti-Auregan, A. et al. Altered astrocyte morphology and vascular development in dystrophin-Dp71-null mice. Glia 64, 716–729 (2016).
- Dorrell, M. I., Aguilar, E. & Friedlander, M. Retinal vascular development is mediated by endothelial filopodia, a preexisting astrocytic template and specific R-cadherin adhesion. *Invest. Ophthalmol. Vis. Sci.* 43, 3500–3510 (2002).
- 27. Bulent Ozpolata, A. et al. Gay, and L. Z. Multiple roles for Pax2 in the embryonic mouse eye. Dev. Biol. 176, 139-148 (2016).
- Chan-Ling, T. et al. Astrocyte-endothelial cell relationships during human retinal vascular development. Invest. Ophthalmol. Vis. Sci. 45, 2020–2032 (2004).
- 29. Babapoor-Farrokhran, S. et al. Angiopoietin-like 4 is a potent angiogenic factor and a novel therapeutic target for patients with proliferative diabetic retinopathy. *Proc. Natl. Acad. Sci. U S A.* **112**, E3030–E3039 (2015).
- Stone, J. et al. Roles of vascular endothelial growth factor and astrocyte degeneration in the genesis of retinopathy of prematurity. *Investig Ophthalmol. Vis. Sci.* 37, 290–299 (1996).
- Yap, L., Tay, H. G., Nguyen, M. T. X., Tjin, M. S. & Tryggvason, K. Laminins in cellular differentiation. Trends Cell. Biol. 29, 987–1000 (2019).
- 32. Yu, Y. et al. Extracellular matrix stiffness regulates microvascular stability by controlling endothelial paracrine signaling to determine pericyte fate. *Arterioscler. Thromb. Vasc Biol.* 43, 1887–1899 (2023).
- 33. Connor, K. M. et al. Quantification of oxygen-induced retinopathy in the mouse: a model of vessel loss, vessel regrowth and pathological angiogenesis. *Nat. Protoc.* 4, 1565–1573 (2009).
- Vähätupa, M., Järvinen, T. A. H. & Uusitalo-Järvinen, H. Exploration of Oxygen-Induced retinopathy model to discover new therapeutic drug targets in retinopathies. Front. Pharmacol. 11, 873 (2020).
- 35. Sun, M. et al. Epithelial membrane protein 2 (EMP2) promotes VEGF-Induced pathological neovascularization in murine Oxygen-Induced retinopathy. *Invest. Ophthalmol. Vis. Sci.* **61**, 3 (2020).
- 36. Guo, Y. et al. Molecular hydrogen promotes retinal vascular regeneration and attenuates neovascularization and neuroglial dysfunction in oxygen-induced retinopathy mice. *Biol. Res.* 57, 43 (2024).
- Bucher, F., Stahl, A., Agostini, H. T. & Martin, G. Hyperoxia causes reduced density of retinal astrocytes in the central avascular zone in the mouse model of oxygen-induced retinopathy. *Mol. Cell. Neurosci.* 56, 225–233 (2013).
- 38. Zhao, K. et al. Celastrol inhibits pathologic neovascularization in oxygen-induced retinopathy by targeting the miR-17-5p/HIF-1a/VEGF pathway. *Cell. Cycle.* 21, 2091–2108 (2022).
- 39. DeNiro, M., Al-Halafi, A., Al-Mohanna, F. H., Alsmadi, O. & Al-Mohanna, F. A. Pleiotropic effects of YC-1 selectively inhibit pathological retinal neovascularization and promote physiological revascularization in a mouse model of oxygen-induced retinopathy. *Mol. Pharmacol.* 77, 348–367 (2010).
- 40. Bosze, B. et al. Multiple roles for Pax2 in the embryonic mouse eye. *Dev. Biol.* **472**, 18–29 (2021).
- 41. Chan-Ling, T., Chu, Y., Baxter, L., Weible Ii, M. & Hughes, S. In vivo characterization of astrocyte precursor cells (APCs) and astrocytes in developing rat retinae: differentiation, proliferation, and apoptosis. *Glia* 57, 39–53 (2009).
- 42. Nyström, A. Laminins in Blood Vessel Development and Disease -Functional Aspects in Angiogenesis, Atherosclerosis, and Muscular Dystrophy (Department of Experimental Medical Science Lund University, 2006).
- 43. Duan, L. J., Pan, S. J., Sato, T. N. & Fong, G. H. Retinal angiogenesis regulates astrocytic differentiation in neonatal mouse retinas by oxygen dependent mechanisms. Sci. Rep. 7, 17608 (2017).
- 44. Park, S. W. et al. Antiangiogenic effect of betaine on pathologic retinal neovascularization via suppression of reactive oxygen species mediated vascular endothelial growth factor signaling. Vascul Pharmacol. 90, 19–26 (2017).
- 45. Zhang, J. et al. HIF-1α and HIF-2α redundantly promote retinal neovascularization in patients with ischemic retinal disease. J. Clin. Invest. 131, (2021).

Author contributions

Xiaoxiao Feng: Performed the experiments, Analyzed the data, Writing-original draft, Writing-review & editing. Changhui Li: Analyzed the data. Kangwei Jiao: Contributed reagents/ materials/analysis tools. Liwei Zhang: Analyzed the data. Wenjia Zhang: Performed the experiments. Yunqing Li: Performed the experiments. Libo Xiao: Performed the experiments, Conceived and designed the experiments, Writing-review & editing.

Funding

This study was supported by the Natural Science Foundation of Yunnan Province [grant numbers 202301AT070241] and Open Research Grants in Ophthalmology, a National Key Clinical Specialty at the Affiliated Hospital of Yunnan University [grant numbers ZKF2024055].

Declarations

Competing interests

The authors declare no competing interests.

Scientific Reports |

Ethics approval

This study was approved by the Ethics Committee of Kunming Medical University (Kmmu20231525) and was conducted according to the ARRIVE guidelines. We confirm that all experiments were performed in accordance with relevant guidelines and regulations.

Additional information

Supplementary Information The online version contains supplementary material available at https://doi.org/1 0.1038/s41598-025-20065-y.

Correspondence and requests for materials should be addressed to L.X.

Reprints and permissions information is available at www.nature.com/reprints.

Publisher's note Springer Nature remains neutral with regard to jurisdictional claims in published maps and institutional affiliations.

Open Access This article is licensed under a Creative Commons Attribution-NonCommercial-NoDerivatives 4.0 International License, which permits any non-commercial use, sharing, distribution and reproduction in any medium or format, as long as you give appropriate credit to the original author(s) and the source, provide a link to the Creative Commons licence, and indicate if you modified the licensed material. You do not have permission under this licence to share adapted material derived from this article or parts of it. The images or other third party material in this article are included in the article's Creative Commons licence, unless indicated otherwise in a credit line to the material. If material is not included in the article's Creative Commons licence and your intended use is not permitted by statutory regulation or exceeds the permitted use, you will need to obtain permission directly from the copyright holder. To view a copy of this licence, visit http://creativecommons.org/licenses/by-nc-nd/4.0/.

© The Author(s) 2025